PCCP

Cite this: *Phys. Chem. Chem. Phys.*, 2011, **13**, 8195–8203

www.rsc.org/pccp

PAPER

Photodissociation dynamics of ClOOCl at 248.4 and 308.4 nm

Wen-Tsung Huang,[ab] Andrew F Chen,[a] I-Cheng Chen,[a] Chen-Hsun Tsai[a] and Jim Jr-Min Lin*[abc]

Received 8th November 2010, Accepted 15th December 2010
DOI: 10.1039/c0cp02453h

The dynamics of ClOOCl photodissociation at 248.4 and 308.4 nm was studied with photofragment translational spectroscopy. At 248.4 nm photoexcitation, the observed products are Cl, O_2, ClO and O. Product translational energy distributions $P(E)$ and anisotropy parameters β were deduced from the measured time-of-flight spectra of the Cl, O_2, and ClO photoproducts. The photodissociation mechanisms have been discussed and compared with available theoretical results. Synchronous and fast sequential breaking of the two Cl–O bonds may both contribute to the dissociation. The relative product yields for [ClO] : [Cl] was measured to be 0.15 ± 0.04 : 1. The relative amounts of [O] : [O_2] products were estimated to be 0.12 : 1. The branching ratios among the Cl + O_2 + Cl : ClO + ClO : ClO + Cl + O product channels were estimated to be 0.82 : 0.08 : 0.10. At 308.4 nm excitation, time-of-flight spectra of the O_2 and ClO photoproducts were recorded while there was interference from Cl_2 impurity in detecting the Cl product. Nonetheless, the observed ClO yield relative to the O_2 yield at 308.4 nm is 1.5 times that at 248.4 nm. The branching ratio between the Cl + O_2 + Cl : ClO + ClO product channels was estimated to be 0.81 : 0.19 at 308.4 nm. This result suggests that the ClO product may contribute a noticeable yield in the photolysis of ClOOCl at the atmospherically important wavelengths above 300 nm.

1. Introduction

The chemical processes responsible for the polar ozone loss are primarily due to two catalytic cycles that involve chlorine and bromine oxides:[1]

(1) ClO dimer cycle:

$$ClO + ClO + M \leftrightarrows ClOOCl + M \quad (1)$$

$$ClOOCl + h\nu \rightarrow 2Cl + O_2 \quad (2)$$

$$2[Cl + O_3 \rightarrow ClO + O_2] \quad (3)$$

$$\text{Net: } 2O_3 + h\nu \rightarrow 3O_2$$

(2) ClO–BrO cycle:

$$BrO + ClO + h\nu \rightarrow Br + Cl + O_2 \quad (4)$$

$$Br + O_3 \rightarrow BrO + O_2 \quad (5)$$

$$Cl + O_3 \rightarrow ClO + O_2 \quad (6)$$

$$\text{Net: } 2O_3 + h\nu \rightarrow 3O_2$$

The ClO dimer cycle has received considerable attention since it was proposed by Molina and Molina[2] in 1987. In current models,[1,3–5] it is crucial for the ozone hole formation. The bottleneck process in this cycle is the Cl-atom production rate J_{Cl} in the photolysis of ClOOCl, which depends on the following three wavelength (λ) dependent factors: (i) the solar flux $I(\lambda)$, (ii) the absorption cross section of ClOOCl $\sigma(\lambda)$, and (iii) the quantum yield of Cl atom production $\phi_{Cl}(\lambda)$.

$$J_{Cl} = \int I(\lambda)\sigma(\lambda)\phi_{Cl}(\lambda)d\lambda \quad (7)$$

A very recent model calculation[4] indicates that the dominant source of model uncertainty in polar ozone loss is uncertainty in the Cl-atom production rate (J_{Cl}) of the ClOOCl photolysis.

The UV absorption spectrum of ClOOCl[6–10] shows a strong and broad feature with a maximum at ~245 nm and a tail which extends to ~400 nm. Since ozone strongly absorbs sunlight at $\lambda < 300$ nm,[10] it is the weak tail of the ClOOCl absorption spectrum at $\lambda > 300$ nm that is responsible for its photodecomposition in the atmosphere. In conventional ClOOCl sample preparations, interference from precursors or byproducts has caused large uncertainties in estimating its concentration and absorption spectrum. This problem is especially severe in the long wavelength region where the ClOOCl absorption is weak.

[a] *Institute of Atomic and Molecular Sciences, Academia Sinica, Taipei 10617, Taiwan. E-mail: jimlin@gate.sinica.edu.tw; Fax: +886 2-23620200*
[b] *Department of Chemistry, National Taiwan University, Taipei 10617, Taiwan*
[c] *Department of Applied Chemistry, National Chiao Tung University, Hsinchu 30010, Taiwan*

In 2007, Pope *et al.*[11] utilized new methods of synthesis and purification of ClOOCl and measured its UV absorption spectrum. These new laboratory data, however, show that the absorption cross section of ClOOCl in the critical wavelength region of $\lambda > 300$ nm is quite small, such that the ClO dimer cycle would contribute much less than that previously thought, implying that the observed ozone loss cannot be explained by existing models.[12]

To resolve the ClOOCl cross section issue, a few groups[13–18] have revisited the absorption cross section of ClOOCl. Among them, Wilmouth *et al.*[14] directly measured the production of Cl atoms from ClOOCl photolysis at 248.4, 308.4 and 351.8 nm. It is worth noting that their data also include the Cl atom quantum yield, not only the absorption cross section.

Our group[16–18] has developed a mass-resolved method to measure the photolysis cross section of ClOOCl. This method does not require a knowledge of the absolute concentration of ClOOCl and precise cross section data can be obtained without interference from impurities. Our results indicate the ClOOCl absorption cross sections are in fact slightly larger than the JPL2006 recommended values.[10] The higher estimate of the photolysis rate of ClOOCl also explains better the field measurements of the [ClOOCl]/[ClO]^2 ratio and the amounts of ozone loss.[3–5,19] Furthermore, it seems that Pope *et al.*[11] misinterpreted their measurements of the ClOOCl cross sections at wavelengths where Cl_2 absorbs and overcorrected the absorbance of the Cl_2 impurity, which may have resulted in too small cross section values for ClOOCl at $\lambda > 300$ nm.

In addition to experimental investigations, there are a number of theoretical studies[20–25] on the ground and excited states of ClOOCl and its absorption spectrum. Quite a few excited states, including singlet and triplet ones,[25] are involved in the absorption from 200 to 400 nm. Due to the complexity of this molecule, however, it is difficult to quantitatively reproduce the experimental absorption spectrum, especially in the long wavelength region.

The UV photodissociation of ClOOCl may lead to the following channels:

$$\mathrm{ClOOCl} + h\nu \rightarrow \mathrm{ClO} + \mathrm{ClO} \qquad 16.3\ \mathrm{kcal\ mol^{-1}} \qquad (8)$$

$$\rightarrow \mathrm{ClOO} + \mathrm{Cl} \qquad 20.4\ \mathrm{kcal\ mol^{-1}} \qquad (9)$$

$$\rightarrow \mathrm{Cl} + \mathrm{O_2} + \mathrm{Cl} \qquad 25.1\ \mathrm{kcal\ mol^{-1}} \qquad (10)$$

$$\rightarrow \mathrm{ClO} + \mathrm{O} + \mathrm{Cl} \qquad 79.7\ \mathrm{kcal\ mol^{-1}} \qquad (11)$$

The threshold energies for channels (8)–(11) (at $T = 0$ K)[26,27] are listed above; the photon energies at 248.4 and 308.4 nm are 115.1 and 92.7 kcal mol^{-1}, respectively. The ClO product from channel (8) would not destroy ozone and ClOOCl can be regenerated through reaction (1),[28] resulting in a null cycle. The ClOO product of channel (9) is very weakly bound ($D_0 = 4.7$ kcal mol^{-1});[29] even a small portion of the available energy will cause its dissociation. Even if stable ClOO is formed, it will dissociate upon thermal collisions in the atmosphere.

$$\mathrm{ClOO} + \mathrm{M} \rightarrow \mathrm{Cl} + \mathrm{O_2} + \mathrm{M} \qquad (12)$$

A high yield of the Cl atom production in the ClOOCl photolysis is evidenced in early bulk studies.[6,30] Due to the complexity of the bulk reaction systems and interference from precursors, error bars of the deduced Cl-atom quantum yields are substantial. Jacobs *et al.*[31] studied the photochemistry and vibrational spectroscopy of Cl_2O_2 isomers isolated in cryogenic matrices. Three isomers, ClOClO, $ClClO_2$, and ClOOCl, have been identified with infrared spectroscopy. For the ClOOCl photolysis, they reported two product channels: (i) ClOO + Cl, resulting in $Cl_2 + O_2$, and (ii) 2ClO, giving rise to ClOClO under the matrix isolation conditions. Moore *et al.*[32] studied the photodissociation of ClOOCl under collision-free conditions in a molecular beam. The branching ratio of Cl *versus* ClO was measured to be $0.88 \pm 0.07 : 0.12 \pm 0.07$ at 248 nm and $0.9 \pm 0.1 : 0.1 \pm 0.1$ at 308 nm. More recently Plenge *et al.*[33] reported detection of the products of ClOOCl photodissociation at 250 and 308 nm with vacuum UV photoionization. They found no evidence of ClO production (yield ≤ 0.02 at 250 nm, ≤ 0.10 at 308 nm) and assigned the photoproducts completely as Cl and O_2, a different observation from Jacobs *et al.*[31] and Moore *et al.*[32] On the other hand, the Cl atom production from the ClOOCl photolysis was probed by Wilmouth *et al.*[14] quite recently. Their Cl-atom product-specific cross sections are 20–30% smaller than our total photolysis cross sections.[16–18] Thus, if we believe both data to be within their error bars, a less-than-unity yield of the $2Cl + O_2$ channel (10) is required to reduce the disparity between them.

Kaledin and Morokuma[22] studied the photodissociation of ClOOCl with classical trajectories where the energy and gradient were computed on the fly by the state-averaged complete active space self-consistent field (CASSCF) calculations. Their results indicate that in the energy regime corresponding to 308 nm excitation, the major dissociation fragments are Cl and O_2, both in the ground state; the higher energy regime of 248 nm excitation yields additional fragments, like ClO, O and ClOO. However, as the authors have mentioned "Given the approximations made in the present study, it is difficult to rate the present results any higher than *qualitative*." Toniolo *et al.*[34] performed a more thorough theoretical study on the same system. Simulations of the nonadiabatic photodissociation dynamics have been run with a direct semiclassical method. They found that dissociation to $2Cl + O_2$ is the main photoreaction, and a small amount of ClO is formed at higher excitation energies (>4.4 eV, <280 nm); the mechanism is mainly sequential at low energies, involving a very short lived species ClOO, while synchronous Cl–O bond breaking prevails at high energies. The quantum yields, translational energy distributions and anisotropy parameters of the photoproducts were computed, aiming to compare with the corresponding experimental quantities.

Previous works[6,14,30–33] are consistent in that the major photoproducts are Cl and O_2. The literature is not consistent in the ClO product yield: there is evidence to support that the ClO channel exists with a noticeable yield,[31,32] but some studies[30,33] have shown a much smaller or zero yield for the ClO product channel. In addition, nowadays the error bars of the cross section measurements have been greatly reduced to about ±5%,[16–18] a better understanding of the ClO quantum yield will improve not only the J_{Cl}-value estimation but also our understanding on the photodissociation dynamics.

2. Experimental

The molecular beam apparatus has been described elsewhere.[35] Only relevant parts of the experiments are given here.

We slightly modified the synthesis method reported by Pope *et al.* (Method 1 of ref. 11) to prepare our ClOOCl sample. The photochemistry is: $Cl_2 + h\nu \rightarrow 2Cl$; $2[Cl + O_3 \rightarrow ClO + O_2]$; $2ClO + M \rightarrow ClOOCl + M$, $M = O_2$. Typically, a gas mixture of Cl_2 ($\sim$0.4%), O_3 ($\sim$6%) and O_2 (balance, 1.1 bar, flow rate $\approx$0.4 l min^{-1}) was introduced into a reaction tube and a pulsed laser beam (355 nm, 80 mJ, 10 Hz) went through the tube to initiate the photoreactions. The reaction temperature was about 200 K; ClOOCl was then condensed in a trapping tube kept at $\sim$150 K. After accumulating ClOOCl for about one hour, we pumped out the reactant gas and let ClOOCl sublimate slowly by warming up the trapping tube to $\sim$153 K. Helium carrier gas (35 Torr) flowed through the trapping tube and carried the ClOOCl through a nozzle (diameter = 0.5 mm, T = 200 K) to form a molecular beam, which lasted for about two hours with a decent intensity. All materials in contact with ClOOCl were fused silica.

The ClOOCl molecular beam was collimated with a skimmer (2 mm diameter, Beam Dynamics, Inc.) and a cryogenic (20 K) aperture (3 mm diameter); the resulted divergence was about $\pm$2.5°. The ClOOCl beam speed centered at 630 m s^{-1} with a width of $\pm$130 m s^{-1}. The photolysis laser beam (excimer laser, KrF: 248.4 nm or XeCl: 308.4 nm, 75 Hz, Lambda Physik LPX210i, 3 × 3 mm^2) intersected with the molecular beam perpendicularly. The photoproducts flew for 24.5 cm and then reached the detector which is equipped with an electron-impact ionizer (70 eV), a quadrupole mass filter, and a Daly-type ion counter. In the analysis, the product time-of-flight (TOF) is defined as the time which a photoproduct spent over the flight distance of 24.5 cm. The molecular beam, laser beam, and detection axis all lay in a horizontal plane as shown in Fig. 1.

For measuring the laser power dependence, we attenuated the laser fluence by a variable attenuator (Laseroptik GmbH, IVA248 or IVA308) of which the reflectivity can be varied by changing the angle of incidence. The transmitted laser beam was partially polarized. The rotation axis of this attenuator was set to 45° away from the vertical direction to obtain a 1 : 1 intensity ratio between the horizontal and vertical polarization components, which is equivalent to a randomly polarized laser beam in our experiments. The average laser power was monitored after the molecular beam chamber with a thermopile power meter (Gentec-EO, UP25N-100H).

For measuring the polarization dependence, linearly polarized laser light was obtained with a set of two thin film polarizer plates (Laseroptik GmbH, TFP248 or TFP308) which reflected the S-polarization and transmitted the P-polarization. The polarization angle was controlled by rotating the polarizer set with a motorized rotating stage (Sigma Koki, SGSP-60YAW-0B). The extinction ratio of the polarizer set was better than 100 : 1.

Typically we accumulated for about 10 000 laser shots to get a raw TOF spectrum and repeated the accumulation a number of times while alternating an experimental parameter like the laser polarization direction back-and-forth to get decent relative intensities and signal-to-noise ratios.

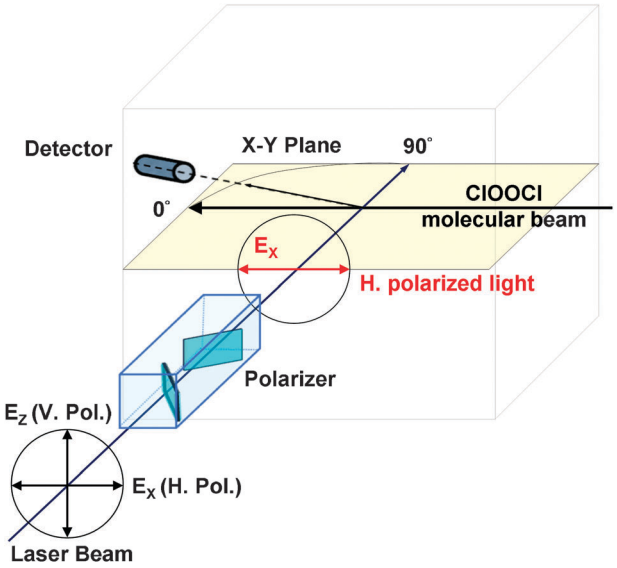

Fig. 1 Scheme of the experimental configuration. The detector can be rotated on the horizontal plane. Both the molecular beam and laser beam are on the detection plane. The direction of the molecular beam defines 0° of the detector angle; the laser beam direction is at 90°.

A TOF spectrum was analyzed with a forward convolution routine which took the instrument functions (*e.g.*, distributions of the beam speed, ionizer length, *etc.*) into account and transformed the data in the laboratory (Lab) frame to those in the center-of-mass (CM) frame.[36] The forward convolution was performed by adjusting the CM-frame translational energy distribution $P(E)$ iteratively until a satisfactory fit to the experimental TOF spectrum was obtained.[37]

The laser polarization dependence was analyzed in the CM frame with the following equation.

$$I(\theta,\phi) = I_0[1 + \beta P_2(\cos\theta)] = I_0[1 + \beta(\tfrac{3}{2}\cos^2\theta - \tfrac{1}{2})] \quad (13)$$

where θ is the angle between the product velocity vector and the laser polarization direction, ϕ is the azimuthal angle; β is the anisotropy parameter, P_2 is the second-order Legendre polynomial.

3. Results and discussion

The synthesis method reported by Pope *et al.* (Method 1 of ref. 11) is effective in producing ClOOCl of a high concentration; most importantly, the only significant impurity is Cl_2. The advantages of this synthesis method have also been confirmed by von Hobe *et al.*[13] Mass scans showed the typical concentration ratios of ClOOCl : Cl_2 : Cl_2O in our molecular beam were about 1 : 0.2–0.5 : 0.001 without any other noticeable impurity. Similar to the observation by Pope *et al.*,[11] the Cl_2 concentration in the sample had some variation.

3.1 Photodissociation at 248.4 nm

At 248.4 nm, Cl_2 has an extremely small absorption cross section ($<10^{-21}$ cm^2)[10] such that we could not detect any Cl atom from Cl_2 photodissociation under all experimental conditions. Since we did not have any significant impurity aside from Cl_2, this became a great advantage over previous

studies—we had no background from photodissociation of impurity or precursors; errors from background subtraction are eliminated.

Fig. 2 shows the product TOF spectra recorded at m/z = 35 (Cl^+) of the ClOOCl photodissociation at 248.4 nm. The Cl^+ TOF spectrum has two distinct peaks showing very different polarization dependences. In our experimental configuration (Fig. 1), the detector probed mainly the parallel component of the dissociation events at the horizontal laser polarization and the perpendicular dissociation component at the vertical laser polarization. The fast peak at m/z = 35 clearly shows preference for the parallel dissociation, while the slow peak shows no polarization dependence at all. Fig. 3 shows the product TOF spectra recorded at m/z = 51 (ClO^+). Since our sample contained no other chlorine oxides than ClOOCl, data in Fig. 3 clearly indicate the production of ClO in the photodissociation. Dissociative ionization of ClO in the electron-impact ionization process would form some Cl^+ as daughter ions. After considering the CM signal intensities at m/z = 35 and 51 as discussed below, we found the predominant part of the m/z = 35 signal is from the Cl atom photoproduct.

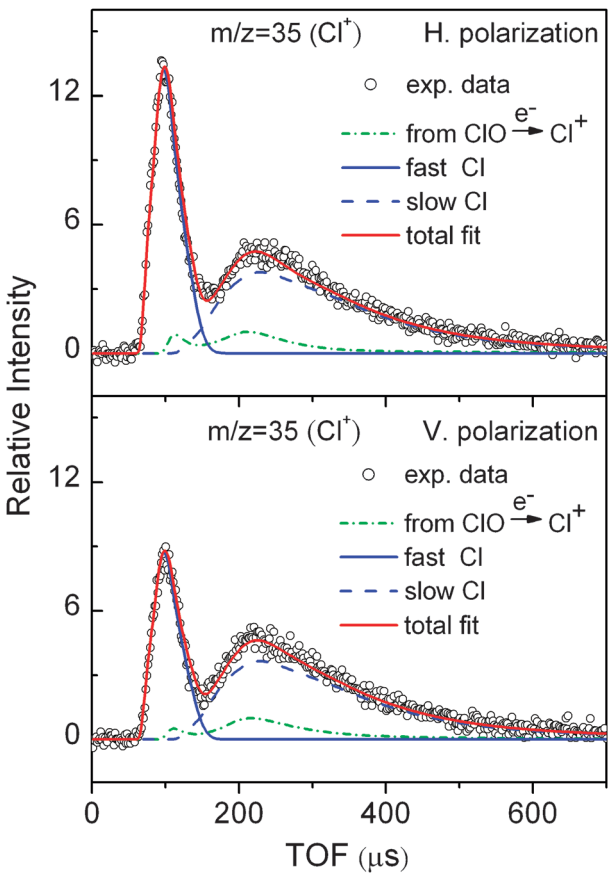

Fig. 2 Product TOF spectra at m/z = 35 (Cl^+) of the ClOOCl photodissociation at 248.4 nm at horizontal (H) and vertical (V) laser polarization directions. The laser pulse energy was about 13 mJ. The detector angle was 20°. The circles are experimental data points; the lines are fits using the CM translational energy distributions $P(E)$ and β parameters shown in Fig. 5 and Table 1. Daughter ions from the ClO photoproduct ($ClO + e^- \rightarrow Cl^+ + O + 2e^-$) are included. See Fig. 1 for the experimental configuration and directions of laser polarization.

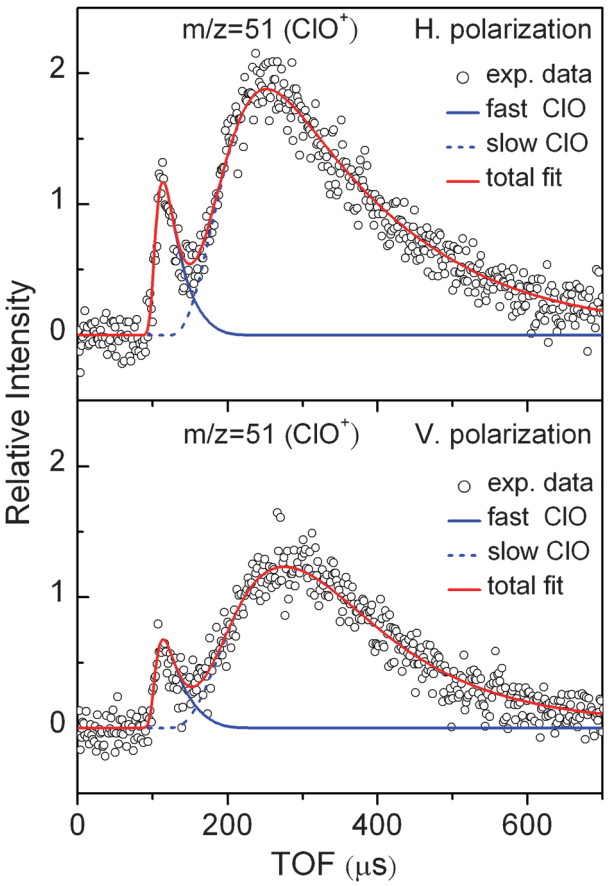

Fig. 3 Product TOF spectra at m/z = 51 (ClO^+) from the ClOOCl photodissociation at 248.4 nm. Other experimental conditions are mentioned in the caption of Fig. 2.

To obtain the relative [ClO] : [Cl] yields, we need to do the following: (i) convert the Lab-frame signal intensities to the CM-frame ones; (ii) calibrate the detection sensitivity of probing Cl *versus* ClO, in which the analysis should include the Cl^+ daughter ions originated from the ClO photoproduct; (iii) consider possible second photon absorption of the ClO product which leads to dissociation to Cl + O.

The CM intensities were obtained by fitting the TOF data at m/z = 35 and 51 using the forward convolution method described in the Experimental section.

The detection sensitivity calibration has been performed with a Cl_2O photolysis experiment at 248.4 nm, which produces momentum-matched ClO + Cl with a fixed 1 : 1 ratio.[32,38,39] In our apparatus, the relative detection sensitivity of ClO (probed at m/z = 51) *versus* Cl (probed at m/z = 35) was measured to be 0.63 : 1. For the ClO product from the Cl_2O photodissociation, the intensity of its Cl^+ daughter ion is about half compared to its parent ion ClO^+. This dissociative ionization accounts for the reduction of the detection sensitivity for ClO (probed at m/z = 51). (Other weaker factors are the electron-impact ionization cross sections and transmission of the quadrupole mass filter.)

The effect of the second photon dissociation has been checked by performing the ClOOCl photolysis experiments at various laser pulse energies from 3 to 30 mJ per pulse. We found the ClO/Cl signal ratio decreases slightly with the laser

energy (~10% per 10 mJ pulse^{-1}), indicating some second photon dissociation of ClO. The final relative yields of [ClO] : [Cl] were determined with an extrapolation of the laser-power-dependent signal ratio of m/z = 51 : m/z = 35 to the zero laser power. (Similar experiments and corrections have also been performed for $Cl_2O + h\nu \rightarrow ClO + Cl$.) After considering all the above factors, the relative quantum yields of [ClO] : [Cl] were determined to be 0.15 ± 0.04 : 1. This result is consistent with Moore *et al.* ([ClO] : [Cl] = 0.14 : 1)[32] but disagrees with Plenge *et al.* ([ClO] : [Cl] < 0.02 : 1).[33]

The O_2 photoproduct was recorded at m/z = 32 (O_2^+) (Fig. 4); only a very fast peak was observed. Interestingly, the O_2 signal is more intense at the vertical polarization than at the horizontal polarization, indicating a negative β value.

Theoretical calculations[22,34] indicate that the ClO + Cl + O product channel (11) may be formed at this excitation energy (~248 nm or ~5 eV). To check the contribution of this channel, we measured the product TOF spectra at m/z = 16 (O^+). In Fig. 4, the main peak of the m/z = 16 signal closely resembles the shape and polarization dependence of the m/z = 32 signal, suggesting that the m/z = 16 signal may just be daughter ions of the O_2 photoproduct. With a more careful examination, a weak bump at ~100 μs is visible in the m/z = 16 TOF spectrum at the horizontal polarization but absent in the m/z = 32 TOF spectra. If we attribute this bump to the

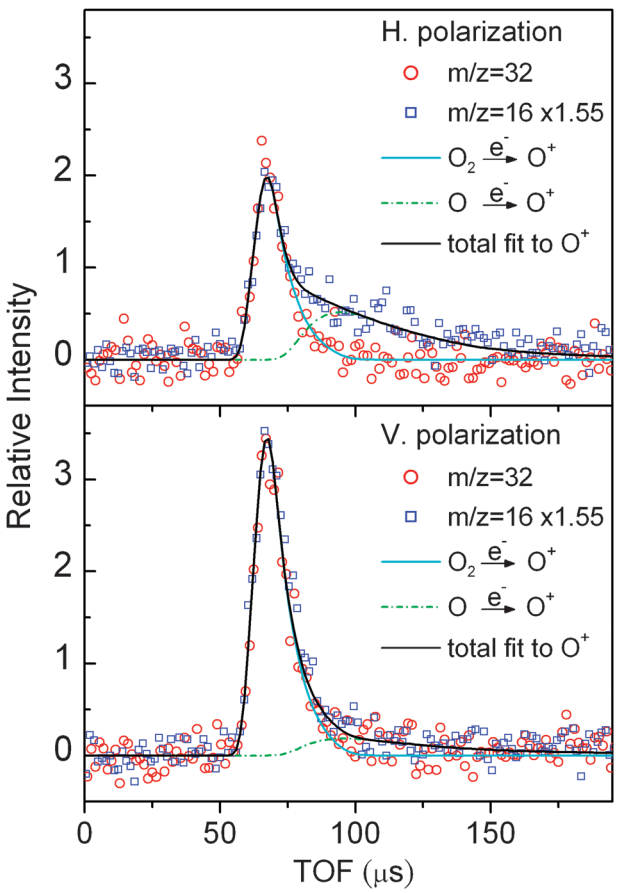

Fig. 4 Product TOF spectra at m/z = 32 and 16 from the ClOOCl photodissociation at 248.4 nm. Other experimental conditions are mentioned in the caption of Fig. 2.

O atom product of channel (11), the relative yields of [O] : [O_2] will be about $0.12^{+0.08}_{-0.02}$: 1. (The range includes the factor of the electron-impact ionization cross sections,[40] and possible variation of the transmission of the quadrupole mass filter. In principle, the transmission is smaller at a higher mass.) If we include the yield of channel (11) in the analysis of the observed [ClO]/[Cl] ratio, the branching ratios of channels (8) : (10) : (11) will become 0.08 : 0.82 : 0.10. Furthermore, the ClOO photoproduct was searched at m/z = 67, but no signal was found.

CM translational energy distributions $P(E)$ and anisotropy parameters β of the Cl, ClO, and O_2 photoproducts were obtained by fitting the experimental data with the forward convolution routine. The best-fit results are shown in Fig. 5 and summarized in Table 1. The O_2 photoproduct has a high velocity and its average translational energy of 34.4 kcal mol^{-1} contributes 38% of the available energy of channel (10). The fast peak of the Cl product covers a broad range of translational energy and it contributes 78% of the total Cl photoproduct. The slow Cl component has a small average translational energy of 2 kcal mol^{-1} and a zero β value. The $P(E)$ of the ClO photoproduct is also bimodal with significant parallel dissociation characters.

It is of no doubt that the ClO and O products are minor in yields and the major photoproducts are Cl and O_2. For the Cl photoproduct, two distinct $P(E)$ distributions indicate at least two distinct sources. At first glance, one might attribute each $P(E)$ distribution to each Cl atom from the two-step reactions of a pure sequential mechanism:

$$ClOOCl + h\nu \rightarrow ClOO^* + Cl \text{ (fast)} \quad (14)$$

$$ClOO^* \rightarrow O_2 + Cl \text{ (slow)} \quad (15)$$

But, the CM intensity of the slow Cl component is much less than that of the fast one, which is not consistent with the mass balance relationship because the excited ClOO* will dissociate completely. On the other hand, if all Cl and O_2 products come from synchronous breaking of the two Cl–O bonds in ClOOCl, it would be difficult to imagine why there is a slow Cl component with β = 0. Furthermore, it may seem unlikely that there are two quite different components of Cl atoms but only one component for O_2. Toniolo *et al.*,[34] however, provided a combination of two mechanisms which seems consistent with our experimental findings. In addition to a synchronous mechanism which produces 2 fast Cl atoms and one fast O_2 molecule, Toniolo *et al.*[34] presented a sequential mechanism that leads to one fast Cl atom, one slow Cl atom, and one fast O_2 molecule. In the sequential mechanism, the second Cl–O bond fission happens after a short time delay of ~60 fs and this delay allows the ClOO fragment to reorientate with the OO group pointing approximately in the forward direction of its initial recoil velocity, and Cl backwards. Therefore, when the second Cl–O bond breaks, the velocity of the center of mass of ClOO adds to that of O_2 and subtracts from that of Cl. Remarkably, the synchronous and sequential O_2 molecules are of similar velocities, resulting in a single peak in the translational energy distribution. A similar situation occurs for the fast Cl atoms from the synchronous and sequential mechanisms. In such a picture, because the slow

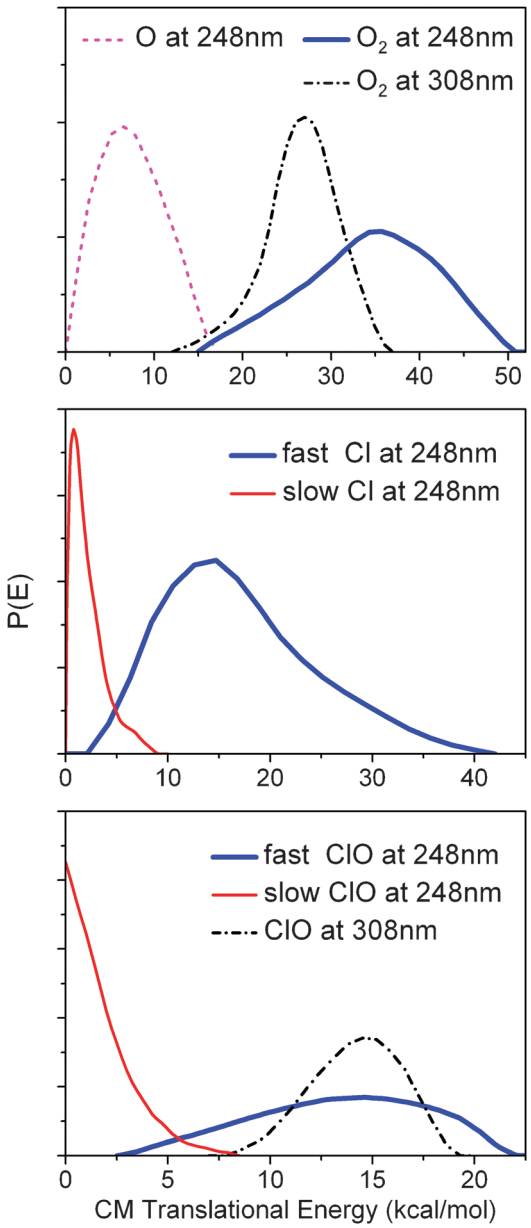

Fig. 5 CM translational energy distributions $P(E)$ for the O_2, O, Cl and ClO photoproducts which were used to fit the experimental TOF spectra of the ClOOCl photodissociation at 248.4 and 308.4 nm. The x-axis scale is for the single-particle translational energy of each photofragment.

Cl only comes from the second step of the sequential mechanism, we may estimate the relative contributions of the synchronous mechanism *versus* the sequential one from the observed ratio of the fast/slow Cl components using the following equation.

$$\frac{2w_{syn} + w_{seq}}{w_{seq}} = \frac{[Cl]_{fast}}{[Cl]_{slow}} = \frac{0.78}{0.22} \qquad (16)$$

where w_{syn} and w_{seq} are the relative weights for the synchronous mechanism and sequential mechanism, respectively. The result is $w_{syn} : w_{seq} = 0.56 : 0.44$. The translational energy release of the synchronous Cl + O_2 + Cl channel is very significant. If we simply add the average translational energies ($\langle E \rangle$ in Table 1) of the 2 fast Cl atoms and the O_2 molecule, we may estimate the total translational energy of the synchronous Cl + O_2 + Cl channel to be $2 \times 17 + 34.4 = 68.4$ kcal mol^{-1}, which is about 76% of the available energy, leaving 21.6 kcal mol^{-1} as the total internal energy. Although the contributions from the minor sequential mechanism will modify the numbers slightly, theoretical calculations[22,34] also indicate large translational energy release for the synchronous mechanism.

The polarization dependences of the Cl and O_2 products may give further clues for the dissociation dynamics. Toniolo *et al.*[34] also calculated the β parameters for both mechanisms. For the O_2 product from the synchronous mechanism, the calculated β is -0.81, but $\beta = +0.33$ for the sequential O_2. The two synchronous Cl atoms and fast sequential Cl atom have β values of 0.91 and 1.19, respectively, while the slow sequential Cl atom has no polarization dependence ($\beta \approx 0$). As discussed above, both synchronous and sequential mechanisms may contribute to the dissociation, thus the resulting β value will be a weighted sum. Our experimental β values shown in Table 1 agree qualitatively with the calculated ones[34] (in correct signs, but the theory overestimates the anisotropy for the fast Cl product). Because quite a few approximations were employed in the calculation,[34] it is hard to be more *quantitative*.

As for the ClO product, its relative yield with respect to the Cl product was measured to be about 0.15 : 1 at 248.4 nm. The calculation of Toniolo *et al.*[34] shows there are a small number of trajectories (10 out of 200) corresponding to the ClO + ClO channel. The theoretical β value for the ClO photoproduct has not been reported yet and the experimental result shows significant anisotropy with positive β values (Table 1). Notably, the same calculation also indicates formation of the electronic excited ClO($A^2\Pi$), although the number of

Table 1 Summary for the observed photoproducts at 248.4 and 308.4 nm

	248.4 nm			308.4 nm	
Photoproduct	Relative weight[a]	$\langle E \rangle$[b]/kcal mol^{-1}	β	$\langle E \rangle$/kcal mol^{-1}	β
Fast Cl	0.78	17.0	0.35 ± 0.03	—[c]	—[c]
Slow Cl	0.22	2.2	0	—[c]	—[c]
O_2	—	34.4	−0.28 ± 0.05	26.6	0.23
Fast ClO	0.55	13.4	0.58 ± 0.04	14.2	0.33
Slow ClO	0.45	1.8	0.55–0.75	—	—
O	—	(7.5)[d]	(0.85)[d]	—	—

[a] Relative weight within the same product. [b] Average translational energy in the CM frame. [c] Contaminated by the photolysis of the Cl_2 impurity. [d] Tentative value.

trajectories is quite limited (6 out of 10). The $A^2\Pi$ state of ClO is known to be predissociative with lifetimes from subpicoseconds to picoseconds.[41]

The slow peak of the $m/z = 51$ TOF spectrum (Fig. 3) may be assigned to the leftover ground state ClO(X) of channel (17).

$$ClOOCl + h\nu \rightarrow ClO\ (X) + ClO\ (A) \rightarrow ClO\ (X) + Cl + O \quad (17)$$

The energy requirement for the formation of ClO(A)[41] + ClO(X) is 106.3 kcal mol^{-1}, which is 8.8 kcal mol^{-1} lower than the photon energy at 248.4 nm. The observed slow ClO component also has low translational energies (see Fig. 5). In addition, the O atom product has been observed with a small yield, in support of channel (17). Another possible assignment for the slow $m/z = 51$ peak is that both ClO are in the electronic ground state but vibrationally and rotationally excited to account for the low translational energies.

Our experimental results are qualitatively consistent with Moore *et al.*[32] but are more definite and precise owing to much improved signal-to-noise ratios and zero background from precursor photolysis. With help from the theoretical calculations,[34] our interpretation of the photodissociation dynamics is a bit different from Moore *et al.*[32]

3.2 Photodissociation at 308.4 nm

The product TOF spectra at $m/z = 32$ (O_2^+) and 51 (ClO^+) of the ClOOCl photodissociation at 308.4 nm are shown in Fig. 6. The $m/z = 32$ TOF spectra at 308.4 and 248.4 nm photolysis wavelengths are quite similar. The available energies for this channel are 90.0 and 67.6 kcal mol^{-1} at 248.4 and 308.4 nm excitations, respectively. On average, the O_2 product carries 38% and 39% of the available energy as its translational energy at 248.4 and 308.4 nm, respectively. This finding suggests similar dissociation mechanisms for the $2Cl + O_2$ channel (10) at both excitation wavelengths.

On the other hand, the $m/z = 51$ TOF spectrum at 308.4 nm shows large differences compared to that at 248.4 nm. First, only the fast peak remains at 308.4 nm; the whole slow peak is missing. In addition, the relative intensity of the $m/z = 51$ peak with respect to the $m/z = 32$ peak is much higher at 308.4 nm than at 248.4 nm. It seems that the higher excited states which are unreachable at 308.4 nm but accessible at 248.4 nm lead to the slow ClO product. The photon energy at 308.4 nm (92.7 kcal mol^{-1}) is not enough to reach the ClO(X) + ClO(A) product state, which may account for the slow ClO peak at 248.4 nm. Furthermore, the ClO + Cl + O channel is not likely to happen in the photodissociation at 308.4 nm because the available energy for this channel is only 13 kcal mol^{-1} but the average translational energy of the ClO + ClO channel is already 28.4 kcal mol^{-1} ($2 \times \langle E \rangle_{ClO}$, which corresponds to 37% of the available energy of the 2ClO channel (8)).

As for the signal at $m/z = 35$ in the 308.4 nm experiment, there is a considerable contribution from the photolysis of Cl_2 impurity (σ_{Cl_2}(308.4 nm) = 1.75×10^{-19} cm^2).[10] To quantitatively subtract out the Cl_2 contribution is an experimental challenge. Without precise data at $m/z = 35$, we could still utilize the signal intensities of the ClO and O_2 photoproducts to obtain the relative yields of the 2ClO channel (8) *versus* the $2Cl + O_2$ channel (10), which have already been determined at 248.4 nm. As discussed above, channels (9) and (11) should not have any yields at 308.4 nm. After the Lab–CM coordinate conversion and corrections for the second photon dissociation, we found the CM intensity ratios of the ClO : O_2 signals are 0.40 ± 0.05 : 1 and 0.60 ± 0.06 : 1 at 248.4 and 308.4 nm, respectively. (It should be noted that the detection sensitivity of O_2 is lower than that of ClO due to its smaller cross section of electron-impact ionization.) This result indicates that the ClO photoproduct at 308.4 nm photolysis is more abundant than at 248.4 nm. The branching ratio of the 2ClO : $2Cl + O_2$ channels at 308.4 nm could be estimated to be 0.19 : 0.81, based on the above determined branching ratios at 248.4 nm.[42] The branching ratio of the $2Cl + O_2$ channel at 248.4 nm is 0.82, very similar to the corresponding value of 0.81 at 308.4 nm; the difference in the overall product yields seems to depend on the opening of the ClO + Cl + O channel.

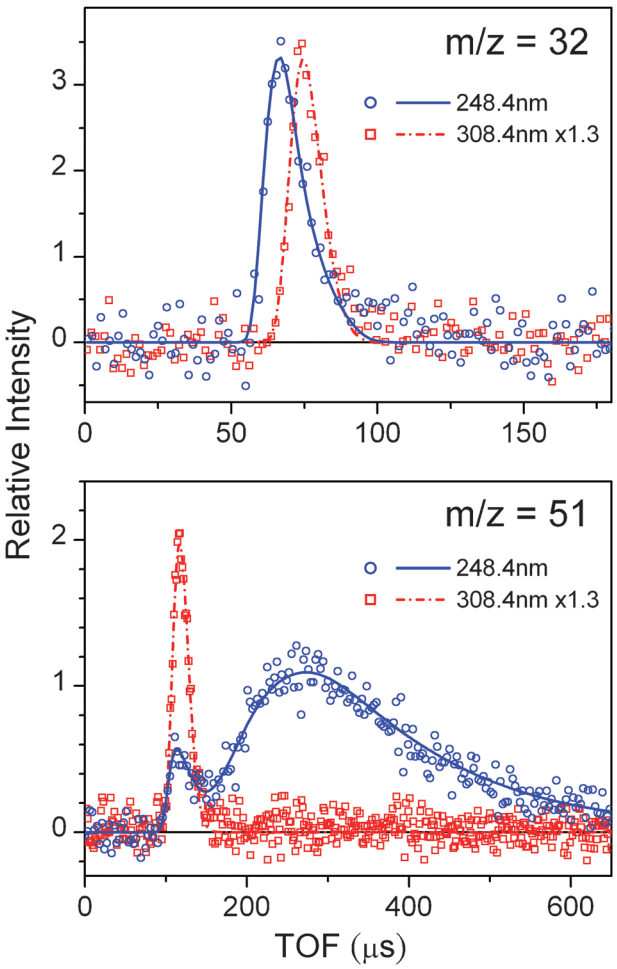

Fig. 6 Product TOF spectra at $m/z = 32$ (O_2^+) and 51 (ClO^+) of the ClOOCl photodissociation at 308.4 nm (laser pulse energy ~89 mJ, polarization angle = 45°, detector angle = 20°). The data accumulation was done in a manner that the two probing masses were alternated back-and-forth. The corresponding TOF spectra of the 248.4 nm photodissociation (laser pulse energy ≈13 mJ) are also shown for comparison.

Theoretical investigations of Kaledin and Morokuma[22] and Toniolo *et al.*[34] found no evidence of the ClO formation in 308 nm photodissociation; the ClO channel was only found at higher energies (~248 nm). Our experimental result, however, is different from the theoretical ones in how the ClO yield changes with the excitation photon energies.

Owing to the small absorption cross section of ClOOCl, small ClO yield, and large interference from precursors, previous studies[6,30] were unable to quantify the ClO yield of ClOOCl photodissociation at 308.4 nm. Moore *et al.*[32] used Cl_2O as a precursor in a similar molecular beam investigation and their ClOOCl photodissociation data were mixed together with the photolysis events of Cl_2O. Despite the difficulties in background subtraction, they reported the ClO : Cl yields to be $0.1 \pm 0.1 : 0.9 \pm 0.1$ at this wavelength. Very recently, Wilmouth *et al.*[14] measured the Cl-atom product-specific cross section of ClOOCl photolysis and our group[16] measured the total photolysis cross section at the same laser wavelengths. In principle, the ratio between these two types of data is the Cl-atom quantum yield. Both groups[14,16] measured the ClOOCl cross section by referencing the experimental data to the known cross sections of other molecules, including Cl_2. If one selects the data[14,16] which were referenced to the Cl_2 cross section, the quantum yield of the $2Cl + O_2$ channel (10) would become 0.79 at 308.4 nm, suggesting the quantum yield of the 2ClO channel (8) is not negligible.

Most ozone depletion models assume production of only ClOO + Cl upon photolysis of ClOOCl.[1] Based on the known experimental results, two points need to be mentioned about this assumption:

(i) There is no evidence of stable ClOO production in the UV photolysis of ClOOCl. Although it does not change any modeling results because of another assumption in the models, $ClOO + M \rightarrow Cl + O_2 + M$, it is incorrect in terms of dissociation mechanism. As the energy of a UV photon is much higher than the threshold energy of channel (10), the dissociation of ClOO should be faster than collision.

(ii) This work indicated that the ClO quantum yield may be noticeable in the ClOOCl photolysis, even in the "atmospheric window" above 300 nm where the most incoming solar radiation occurs.

4. Conclusions

The photodissociation dynamics of ClOOCl has been studied at 248.4 and 308.4 nm. Improved sample purity has allowed us to probe the dynamics more clearly, especially for the minor product channels. At both wavelengths, Cl and O_2 are the major products while ClO has been definitely observed with noticeable yields. Contrary to theoretical predictions,[22,34] we found a higher ClO product yield at 308.4 nm than at 248.4 nm. This observation has opened a new question—*Does the ClO quantum yield become larger at wavelengths longer than 308 nm*?

At 248.4 nm excitation the Cl product has a fast component and a slow component. The fast component favors parallel dissociation while the slow component has no polarization dependence. The O_2 product has a high translational energy release and favors perpendicular dissociation. The ClO product has a bimodal energy distribution with positive β values. Some minor amount of O atom has been observed, indicating existence of the ClO + Cl + O product channel. Analysis of $P(E)$ and β values of the Cl and O_2 products indicates the synchronous and sequential mechanisms proposed by Toniolo *et al.*[34] may be qualitatively valid. At 308.4 nm excitation, the O_2 formation dynamics is similar to that at 248.4 nm, but the ClO + ClO channel exhibits quite different and simpler dynamics.

Acknowledgements

This work was supported by Academia Sinica and the National Science Council of Taiwan (NSC 98-2113-M-001-027-MY2). The authors thank Prof. Yuan T. Lee for valuable comments.

Notes and references

1 World Meteorological Organization (WMO), Scientific Assessment of Ozone Depletion: 2006, Global research and monitoring project—Report No. 50, (WMO, Geneva, Switzerland, 2007); http://ozone.unep.org/Assessment_Panels/SAP/Scientific_Assessment_2006.
2 L. T. Molina and M. J. Molina, *J. Phys. Chem.*, 1987, **91**, 433.
3 K. Frieler, M. Rex, R. J. Salawitch, T. Canty, M. Streibel, R. M. Stimpfle, K. Pfeilsticker, M. Dorf, D. K. Weisenstein and S. Godin-Beekmann, *Geophys. Res. Lett.*, 2006, **33**, L10812.
4 S. R. Kawa, R. S. Stolarski, P. A. Newman, A. R. Douglass, M. Rex, D. J. Hofmann, M. L. Santee and K. Frieler, *Atmos. Chem. Phys.*, 2009, **9**, 8651.
5 M. von Hobe, R. J. Salawitch, T. Canty, H. Keller-Rudek, G. K. Moortgat, J.-U. Groos, R. Müller and F. Stroh, *Atmos. Chem. Phys.*, 2007, **7**, 3055.
6 R. A. Cox and G. D. Hayman, *Nature*, 1988, **332**, 796.
7 J. B. Burkholder, J. J. Orlando and C. J. Howard, *J. Phys. Chem.*, 1990, **94**, 687.
8 W. B. DeMore and E. Tschuikow-Roux, *J. Phys. Chem.*, 1990, **94**, 5856.
9 K. J. Huder and W. B. DeMore, *J. Phys. Chem.*, 1995, **99**, 3905.
10 S. P. Sander, B. J. Finlayson-Pitts, R. R. Friedl, D. M. Golden, R. E. Huie, H. Keller-Rudek, C. E. Kolb, M. J. Kurylo, M. J. Molina, G. K. Moortgat, V. L. Orkin, A. R. Ravishankara and P. H. Wine, *Chemical Kinetics and Photochemical Data for Use in Atmospheric Studies 06-2*, Jet Propulsion Laboratory, Pasadena, 2006.
11 F. D. Pope, J. C. Hansen, K. D. Bayes, R. R. Friedl and S. P. Sander, *J. Phys. Chem. A*, 2007, **111**, 4322.
12 M. von Hobe, *Science*, 2007, **318**, 1878.
13 M. von Hobe, F. Stroh, H. Beckers, T. Benter and H. Willner, *Phys. Chem. Chem. Phys.*, 2009, **11**, 1571.
14 D. M. Wilmouth, T. F. Franco, R. M. Stimpfle and J. G. Anderson, *J. Phys. Chem. A*, 2009, **113**, 14099.
15 D. K. Papanastasiou, V. C. Papadimitriou, D. W. Fahey and J. B. Burkholder, *J. Phys. Chem. A*, 2009, **113**, 13711.
16 H.-Y. Chen, C.-Y. Lien, W.-Y. Lin, Y. T. Lee and J. J. Lin, *Science*, 2009, **324**, 781.
17 C.-Y. Lien, W.-Y. Lin, H.-Y. Chen, W.-T. Huang, B. Jin, I.-C. Chen and J. J. Lin, *J. Chem. Phys.*, 2009, **131**, 174301.
18 B. Jin, I.-C. Chen, W.-T. Huang, C.-Y. Lien, N. Guchhait and J. J. Lin, *J. Phys. Chem. A*, 2010, **114**, 4791.
19 R. M. Stimpfle, D. M. Wilmouth, R. J. Salawitch and J. G. Anderson, *J. Geophys. Res., [Atmos.]*, 2004, **109**, D03301.
20 F. Jensen and J. Oddershede, *J. Phys. Chem.*, 1990, **94**, 2235.
21 J. F. Stanton and R. J. Bartlett, *J. Chem. Phys.*, 1993, **98**, 9335.
22 A. L. Kaledin and K. Morokuma, *J. Chem. Phys.*, 2000, **113**, 5750.
23 A. Toniolo, M. Persico and D. Pitea, *J. Phys. Chem. A*, 2000, **104**, 7278.
24 P. Tomasello, M. Ehara and H. Nakatsuji, *J. Chem. Phys.*, 2002, **116**, 2425.

25 K. A. Peterson and J. S. Francisco, *J. Chem. Phys.*, 2004, **121**, 2611.
26 J. D. Cox, D. D. Wagman and V. A. Medvedev, *CODATA Key Values for Thermodynamics*, Hemisphere, New York, 1989.
27 M. W. Chase Jr., C. A. Davies, J. R. Downey Jr., D. J. Frurip, R. A. McDonald and A. N. Syverud, JANAF Thermochemical Tables (Third Edition), *J. Phys. Chem. Ref. Data*, 1985, **14**(suppl. 1), 1.
28 V. Ferracci and D. M. Rowley, *Phys. Chem. Chem. Phys.*, 2010, **12**, 11596.
29 K. Suma, Y. Sumiyoshi, Y. Endo, S. Enami, S. Aloisio, S. Hashimoto, M. Kawasaki, S. Nishida and Y. Matsumi, *J. Phys. Chem. A*, 2004, **108**, 8096.
30 M. J. Molina, A. J. Colussi, L. T. Molina, R. N. Schindler and T.-L. Tso, *Chem. Phys. Lett.*, 1990, **173**, 310.
31 J. Jacobs, M. Kronberg, H. S. P. Müller and H. Willner, *J. Am. Chem. Soc.*, 1994, **116**, 1106.
32 T. A. Moore, M. Okomura, J. W. Seale and T. K. Minton, *J. Phys. Chem.*, 1999, **103**, 1691.
33 J. Plenge, R. Flesch, S. Kuhl, B. Vogel, R. Muller, F. Stroh and E. Ruhl, *J. Phys. Chem. A*, 2004, **108**, 4859.
34 A. Toniolo, G. Granucci, S. Ingleseb and M. Persico, *Phys. Chem. Chem. Phys.*, 2001, **3**, 4266.
35 J. J. Lin, D. W. Hwang, S. Harich, Y. T. Lee and X. Yang, *Rev. Sci. Instrum.*, 1998, **69**, 1642.
36 R. K. Sparks, K. Shobatake, L. R. Carlson and Y. T. Lee, *J. Chem. Phys.*, 1981, **75**, 3838.
37 K. T. Gillen and B. H. Mahan, *J. Chem. Phys.*, 1972, **56**, 2517.
38 C. M. Nelson, T. A. Moore, M. Okumura and T. K. Minton, *J. Chem. Phys.*, 1994, **100**, 8055.
39 T. A. Moore, M. Okumura and T. K. Minton, *J. Chem. Phys.*, 1997, **107**, 3337.
40 http://physics.nist.gov/PhysRef Data/Ionization/.
41 W. H. Howie, I. C. Lane, S. M. Newman, D. A. Johnson and A. J. Orr-Ewing, *Phys. Chem. Chem. Phys.*, 1999, **1**, 3079.
42 In principle, the detection efficiencies of ClO (probed at $m/z = 51$) and O_2 (probed at $m/z = 32$) should depend on their internal states to some extent. The rotational and vibrational excitations affect very little the total cross section of electron impact ionization because the energy used in the electron impact ionization is about 70 eV, much higher than the internal energies of the molecules. But these internal excitations would affect the probability of dissociative ionization and thus the signal ratios among daughter ions and the parent ions. Because an electronic excited state usually has a lifetime much shorter than our detection time scale, we do not need to worry about electronic excitations. For detecting ClO *versus* Cl, our calibration was performed *via* $Cl_2O + h\nu \rightarrow Cl + ClO$, in which the ClO product has a broad internal energy distribution. Nonetheless, based on ref. 38 in which an energy-independent ionic fragmentation can fit the experimental data well, we believe that the daughter ion formation of ClO should not depend on its internal energy strongly. In addition, if the ClO from the ClOOCl photolysis has a similar distribution of internal energy, the effect of internal energy may be canceled in our calibration process. If not fully canceled, we estimate this effect should be in the order of 25%, based on possible variation of the daughter ion yield.